

Magnetic circular x-ray dichroism study of $\text{La}_{1-x}\text{Sr}_x\text{CoO}_3$

J. Okamoto,¹ H. Miyauchi,² T. Sekine,² T. Shidara,³ T. Koide,² K. Amemiya,⁴ A. Fujimori,^{1,5} T. Saitoh,² A. Tanaka,⁶ Y. Takeda,⁷ and M. Takano⁸

¹Department of Physics, University of Tokyo, Bunkyo-ku, Tokyo 113-0033, Japan

²Photon Factory, IMSS, High Energy Accelerator Research Organization, Tsukuba, Ibaraki 305-0801, Japan

³Accelerator Research Laboratory, High Energy Accelerator Research Organization, Tsukuba, Ibaraki 305-0801, Japan

⁴Department of Chemistry, University of Tokyo, Bunkyo-ku, Tokyo 113-0033, Japan

⁵Department of Complexity Science and Engineering, University of Tokyo, Bunkyo-ku, Tokyo 113-0033, Japan

⁶Department of Materials Science, Faculty of Science, Hiroshima University, Higashi-Hiroshima 739-8526, Japan

⁷Department of Chemistry, Faculty of Engineering, Mie University, Tsu 514-0008, Japan

⁸Institute for Chemical Research, Kyoto University, Uji, Kyoto 611-0011, Japan

(Received 17 November 1999; revised manuscript received 14 April 2000)

The ferromagnetic oxide $\text{La}_{1-x}\text{Sr}_x\text{CoO}_3$ has been studied by magnetic circular x-ray dichroism (MCXD) in core-level absorption. In the Co $2p_{3/2,1/2}$ absorption, the orbital and spin magnetic moments of the Co $3d$ are deduced with the use of magneto-optical sum rules and compared with magnetization measurements. In the O $1s$ absorption, large negative MCXD structures are observed, showing that the O $2p$ orbitals are heavily mixed with the Co $3d$ orbitals and that the orbital magnetic moment of O $2p$ is parallel to the orbital magnetic moment of Co $3d$ and the total magnetic moment. The relative magnitudes of the spin and orbital magnetic moments are most consistently interpreted based on the intermediate-spin states of Co $3d$ within the ionic model, although the absolute values of the spin and orbital magnetic moments are found to be smaller, probably indicating that the itinerant electron description of the Co $3d$ states is more appropriate in $\text{La}_{1-x}\text{Sr}_x\text{CoO}_3$.

I. INTRODUCTION

$3d$ transition-metal (TM) oxides have interested many researchers for their various electronic and magnetic properties. LaCoO_3 , which crystallizes in the rhombohedrally distorted perovskite structure, is a charge-transfer-type semiconductor¹ with a transport gap of ~ 0.6 eV (Ref. 2) and is nonmagnetic at low temperatures. However, it becomes paramagnetic above ~ 90 K and metallic above ~ 500 K.³⁻⁵ The ground state of the Co^{3+} ion is thought to take the low-spin (LS) state $^1A_1 (t_{2g}^6)$. The temperature-induced paramagnetism is thought to originate from the mixing of the LS ground state with magnetic excited states⁷ such as the high-spin (HS) $^5T_2 (t_{2g}^4 e_g^2)$ and the intermediate-spin (IS) $^3T_1 (t_{2g}^5 e_g^1)$ states, but the spin states at high temperatures still remain controversial: the transition at 90 K has been attributed to the LS to HS transition^{8,9} or the transition at 500 K to the LS to HS one;^{5,6,10,11} alternatively, the 90 K transition has been attributed to the LS to IS transition.¹² Hole-doped LaCoO_3 , namely $\text{La}_{1-x}\text{Sr}_x\text{CoO}_3$, also shows various magnetic and electronic properties as functions of doped hole concentration x . Sr doping remarkably increases the magnetization and the system changes from the nonmagnetic semiconductor to a ferromagnetic metal for $x \geq 0.2$.^{2-4,6,13-15} Itoh *et al.* showed that $\text{La}_{1-x}\text{Sr}_x\text{CoO}_3$ with $0 < x \leq 0.18$ at low temperatures ($\sim 10-50$ K) takes a spin-glass state.^{13,16} The spin-glass state in $\text{La}_{0.92}\text{Sr}_{0.08}\text{CoO}_3$ was observed in a neutron-scattering study below ~ 24 K.⁸ The Curie temperature T_C increases monotonically with increasing x and reaches a maximum of 280 K at $x \approx 0.7$, and then decreases linearly with x to 220 K at $x = 1$.^{17,18} As for the electronic

structure of the Co $3d$ states in $\text{La}_{1-x}\text{Sr}_x\text{CoO}_3$, different spin states, LS, IS, and HS states, have been considered, and it has been controversial which spin states are realized. From magnetization measurements, Taguchi *et al.*¹⁷ have concluded that superexchange interaction for $\text{Co}^{3+}-\text{O}-\text{Co}^{4+}$ is stronger than those for $\text{Co}^{4+}-\text{O}-\text{Co}^{4+}$ and $\text{Co}^{3+}-\text{O}-\text{Co}^{3+}$ and that the Co^{3+} and Co^{4+} ions are in the high- and low-spin states, respectively. Potze *et al.*¹⁹ have argued that the Co^{4+} ion in SrCoO_3 is in the intermediate-spin state because the d^6L configuration dominates the ground state from the line shape of the Co $2p$ x-ray-absorption (XAS) spectrum. A recent photoemission and x-ray-absorption spectroscopic study of $\text{La}_{1-x}\text{Sr}_x\text{CoO}_3$ has suggested that the intermediate-spin state is realized in the ferromagnetic phase.²⁰

Magnetic circular x-ray dichroism (MCXD) in core-level soft-x-ray absorption is a powerful method to obtain information about the magnetic states at each atomic site. With use of magneto-optical sum rules, it gives the orbital magnetic moment and the spin magnetic moment on each atom. In this paper, $\text{La}_{1-x}\text{Sr}_x\text{CoO}_3$ has been studied by MCXD at low temperature (40 K) under a magnetic field (2 T) and the result is compared with that of magnetization measurements. Based on the orbital and spin magnetic moments in the Co $3d$ states and the orbital magnetic moment in the O $2p$ states deduced here, discussion is made about the spin state of the Co $3d$ states in $\text{La}_{1-x}\text{Sr}_x\text{CoO}_3$.

II. EXPERIMENT

Polycrystalline samples of $\text{La}_{1-x}\text{Sr}_x\text{CoO}_3$ were prepared by the following procedure.²⁰ Sintered mixtures of appropri-

ate molar quantities of La_2O_3 , SrCO_3 , and Co_3O_4 were pressed into pellets. For LaCoO_3 , $\text{La}_{0.9}\text{Sr}_{0.1}\text{CoO}_3$, and $\text{La}_{0.2}\text{Sr}_{0.2}\text{CoO}_3$, pellets were fired in an O_2 atmosphere at 900°C for 48 h, at 1200°C for 24 h, and at 1300°C for 24 h, and then slowly cooled to room temperature. For $\text{La}_{0.6}\text{Sr}_{0.4}\text{CoO}_3$ and $\text{La}_{0.4}\text{Sr}_{0.6}\text{CoO}_3$, pellets were further annealed under an O_2 pressure of 300 atm at 350°C for 82 h after the above process. For $\text{La}_{0.2}\text{Sr}_{0.8}\text{CoO}_{3-\delta}$ and $\text{SrCoO}_{3-\delta}$, where δ was $\sim 0.05-0.1$, pellets were fired at 1300°C in a N_2 gas flow, quenched into liquid N_2 , and annealed under an O_2 pressure of 200 atm at 350°C for about a week. Each sample was checked to be single phase by x-ray diffraction.

MCXD measurements were made in the total-electron-yield mode using circularly polarized synchrotron radiation from the bending-magnet beam line BL-11A at the Photon Factory, High Energy Accelerator Research Organization. The measurements were carried out at 40 ± 0.1 K, which is well below T_C (Refs. 6,16,18) for the $x \geq 0.2$ samples. The sample chamber was kept at $(2-3) \times 10^{-10}$ Torr. The sample surface was cleaned by *in situ* scraping before each series of measurement. Magnetic fields of ± 2 T, which were enough to magnetize the samples, were applied to the sample using a superconducting magnet. The photon helicity was fixed and the magnetic field direction was reversed parallel and antiparallel to it. For each x , we performed several sets of MCXD measurements and error bars were estimated from the reproducibility of the MCXD spectra. The degree of circular polarization (P_c) was estimated to be $(74 \pm 4)\%$ by comparison of measured Ni and Co $2p$ MCXD of Ni and Co metal with reported MCXD intensities.^{21,22} The incident photon flux was monitored using an Au mesh placed down the beamline of the postfocusing mirror. We have also measured the magnetization by a SQUID magnetometer for samples which were cut out of the same pellet that were used in the MCXD measurement under the same experimental condition ($B = 2$ T, $T = 40$ K). As for the $x = 0$ sample, the magnetization was nearly zero ($\leq 10m\mu_B$)

III. RESULTS AND DISCUSSIONS

Figure 1(a) shows the Co $2p$ XAS spectrum $(\mu^+ + \mu^-)/2$ and the background for $\text{La}_{1-x}\text{Sr}_x\text{CoO}_3$ ($x = 0.4$), and Fig. 1(b) shows the photon flux-normalized polarization-dependent Co $2p$ XAS spectra μ^+ and μ^- for $\text{La}_{1-x}\text{Sr}_x\text{CoO}_3$. Here, μ^+ and μ^- refer to the absorption coefficients for photon helicity parallel and antiparallel to the Co $3d$ majority-spin direction, respectively. MCXD spectra ($\Delta\mu = \mu^+ - \mu^-$) and their energy integrals are shown in Fig. 1(c). Each MCXD spectrum has been corrected for P_c . The background curve corresponds to the transition from the Co $2p$ levels to the continuum. As for the background for μ^+ and μ^- , we have assumed a broadened step function, as shown in Fig. 1(a), i.e., an arctangent function whose step height was set 2:1 for Co $2p_{3/2}$ and Co $2p_{1/2}$ and step energies were set at the peaks of the Co $2p_{3/2}$ transition (~ 779.3 eV) and the Co $2p_{1/2}$ transition (~ 794 eV) for each x . In the ferromagnetic region ($0.2 \leq x \leq 1.0$), large MCXD structures were observed, while only very weak structures were observed in the spin-glass ($x = 0.1$) samples. In the case of the $x = 0$ sample, the weak structures around the Co $2p_{3/2}$

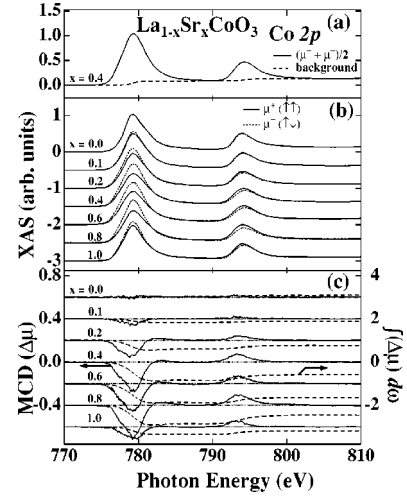


FIG. 1. (a) Co $2p$ XAS spectrum $(\mu^+ + \mu^-)/2$ and the background for $x = 0.4$, and (b) μ^+ and μ^- spectra of $\text{La}_{1-x}\text{Sr}_x\text{CoO}_3$. The spectra have been normalized to the Co $2p_{3/2}$ peak height, from which background has been subtracted. (c) Co $2p$ MCXD spectra and their energy integrals. Corrections for the degree of circular polarization P_c of the incident light have been made.

and the $2p_{1/2}$ peaks were not fully reproducible. Therefore, we shall not discuss the $x = 0$ data in the following analysis.

From these spectra, the orbital magnetic moment M_{orb} and the spin magnetic moment M_{spin} of the Co $3d$ states in the ground state were estimated with use of the MCXD orbital sum rule²³ and spin sum rule²⁴

$$M_{\text{orb}} = -2 \frac{\Delta A_{L_3} + \Delta A_{L_2}}{3(A_{L_3} + A_{L_2})} (10 - N_{3d}), \quad (1)$$

$$M_{\text{spin}} + 7M_T = -\frac{\Delta A_{L_3} - 2\Delta A_{L_2}}{A_{L_3} + A_{L_2}} (10 - N_{3d}), \quad (2)$$

where M_{orb} , M_{spin} , and the magnetic-dipole moment M_T are in units of μ_B/atom , N_{3d} is the $3d$ electron occupation number, ΔA_{L_3} and ΔA_{L_2} are the energy-integrated $2p_{3/2}$ and $2p_{1/2}$ MCXD intensities (up to $h\nu \sim 810$ eV in the case of the Co $2p$ core level), respectively, and A_{L_3} and A_{L_2} are the energy-integrated $2p_{3/2}$ and $2p_{1/2}$ XAS intensities. In estimating the spin magnetic moments from the XAS and MCD spectra, we have to separate the Co $2p_{3/2}$ component and the Co $2p_{1/2}$ component. We divided the Co $2p$ spectra into two components at ~ 790 eV, where the difference between the XAS intensity and background becomes the smallest as shown in Fig. 1(a), and the overlap of the Co $2p_{3/2}$ and the Co $2p_{1/2}$ components is considered to be the smallest. In all the samples, except $x = 0$, $\Delta A_{L_3} + \Delta A_{L_2}$ are seen to take negative finite values. This means that $M_{\text{orb}} > 0$ and $M_{\text{spin}} > 0$, which is normally expected for a more-than-half-filled d -electron shell.

The orbital M_{orb} , spin M_{spin} , and the total $M_{\text{tot}} = M_{\text{orb}} + M_{\text{spin}}$ magnetic moments estimated using the above sum rules are compared with the magnetization measured by a SQUID magnetometer in Fig. 2(a). As for the spin sum rule, the magnetic-dipole moment M_T in Eq. (2) is estimated to be very small ($\leq 1\%$ of M_{spin}) in a ligand-field theoretical

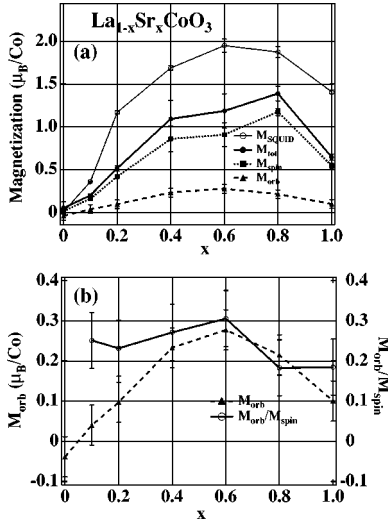


FIG. 2. (a) Orbital M_{orb} , spin M_{spin} , and total M_{tot} magnetic moments per Co atom obtained from the MCXD orbital (Ref. 23) and spin sum rules (Ref. 24) as functions of x . The total magnetic moment obtained from the SQUID measurements (M_{SQUID}) are values at $B=2$ T and $T=40$ K as in the MCXD measurements. (b) Ratio M_{orb}/M_{spin} and M_{orb} per Co atom.

calculation.²⁵ Furthermore, our measurements were made on polycrystals, fulfilling an angle average with the resultant vanishing magnetic-dipole term.²⁶ N_{3d} was deduced to be 6.8 for $x=0$ and 5.8 for $x=1$ obtained from the cluster-model analyses.^{12,27} N_{3d} for other x were determined from the N_{3d} of $x=0$ and 1 by $N_{3d}(x) = 6.8 \times (1-x) + 5.8 \times x$. The x dependence of the MCXD M_{tot} qualitatively agrees well with that of the magnetization M_{SQUID} . This means that our MCXD measurements and subsequent analyses have given reasonable results. As for the absolute value of the total magnetic moments, however, the MCXD M_{tot} is 30–40% smaller than M_{SQUID} . There are two possible reasons for this observation. First, we should take into account the correction factor for the spin sum rule [Eq. (2)] pointed out by Teramura *et al.*²⁵ From their ligand-field theoretical calculation, the magnitude of the correction factor was obtained to be 20–30% of MCXD M_{spin} . Thus, even if the correction has been taken into account, a finite discrepancy of 10–20% still remains between M_{tot} and M_{SQUID} . Second, the magnetic moments of the O $2p$ orbitals contribute somewhat to M_{tot} . It is thought that magnetic moments are induced on the O $2p$ orbitals as a result of mixing with the Co $3d$ orbitals. MCXD M_{orb} and PES measurements^{12,27} show that a rather large amount of charges (nearly one electron) is transferred from the ligand O $2p$ orbitals to the Co $3d$ orbitals, resulting in a net magnetization of the O $2p$ orbitals.

The ratio M_{orb}/M_{spin} is plotted as a function of x in Fig. 2(b). Though there is a weak peak at $x=0.6$, the ratio gradually decreases with x , which may be most naturally explained by the increasing itinerancy with x . In considering the electronic and magnetic states of the Co ion in $\text{La}_{1-x}\text{Sr}_x\text{CoO}_3$, we compare the experimentally deduced magnetic moments with those predicted by the ionic model, where three different spin states are considered for the Co^{3+} and Co^{4+} ions. The M_{orb} , M_{spin} , and M_{orb}/M_{spin} for each spin state thus predicted are given in Table I. From this information and the

TABLE I. Orbital M_{orb} and spin M_{spin} magnetic moment of the Co atom in $\text{La}_{1-x}\text{Sr}_x\text{CoO}_3$ (in units of μ_B/Co) and the ratio M_{orb}/M_{spin} according to the ionic model (Refs. 25 and 29).

Spin state	x	M_{orb}	M_{spin}	M_{orb}/M_{spin}
LS	0 (Co^{3+})	0	0	
	1 (Co^{4+})	0.859	0.384	2.236
IS	0 (Co^{3+})	≈ 1	~ 2	≈ 0.5
	1 (Co^{4+})	≈ 1	~ 3	≈ 0.33
HS	0 (Co^{3+})	0.711	3.3	0.215
	1 (Co^{4+})	0.01	4.96	

experimental values of M_{orb}/M_{spin} , ~ 0.25 and ~ 0.2 for $x=0.1$ and 1, respectively, the IS state is thought to be most likely for the electronic states of the Co $3d$ ion throughout $0.2 \leq x \leq 1$. However, the absolute values of M_{spin} and M_{orb} are significantly smaller than the prediction of the ionic model. In order to explain this, the itinerant electron description of the Co $3d$ states may be necessary for $\text{La}_{1-x}\text{Sr}_x\text{CoO}_3$.

In order to investigate the magnetic properties projected on the O $2p$ orbitals, we have also made the MCXD measurements for the O $1s$ XAS spectra. Figures 3(a) and 3(b) show the photon flux-normalized μ^+ and μ^- O $1s$ XAS spectra of $\text{La}_{1-x}\text{Sr}_x\text{CoO}_3$. The average of the μ^+ and μ^- spectra has been normalized to 1 at the first peak. The O $1s$ XAS spectra come from the unoccupied states mixed with the O $2p$ unoccupied states: the Co $3d$ states in the region of 524–530 eV, the La $5d$ or Sr $4d$ states in the region of 530–537 eV, and the Co $4sp$ states in the region of 537–545 eV. The difference between the μ^+ and μ^- spectra is systematic and relatively large in the Co $3d$ region but small in the La $5d$ /Sr $4d$ region and the Co $4sp$ region. Since appreciable MCD structures were observed in the Co $3d$ region and the magnetic moments in the O $2p$ states are thought to be caused by the charge transfer to the Co $3d$ states, we consider only the Co $3d$ region of the O $1s$ XAS spectra in estimating the magnetic effects in the O $2p$ states as shown in Figs. 3(b) and 3(c). The O $1s$ MCXD spectra and their energy integrals are shown in Fig. 3(c). The MCXD

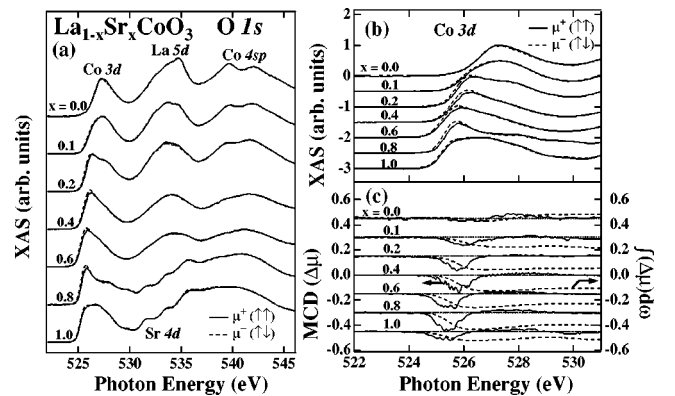


FIG. 3. O $1s$ XAS spectra, μ^+ and μ^- , of $\text{La}_{1-x}\text{Sr}_x\text{CoO}_3$ in wide energy range (a) and in the threshold region (b). The spectra have been normalized to the average $[(\mu^+ + \mu^-)/2]$ first-peak height. (c) O $1s$ MCXD spectra and their energy integrals. Corrections for P_c have been made.

signals in the Co 3*d* region (524–530 eV) are 10–15 % of the O 1*s* XAS peak height and the energy integrals up to ~530 eV are negative for the ferromagnetic samples ($0.2 \leq x \leq 1$). In another perovskite-type 3*d* TM oxide system $\text{La}_{1-x}\text{Sr}_x\text{MnO}_3$, the ratio of the MCXD signal to the XAS one in the O 1*s* absorption region is $\leq 10\%$.²⁸ This may indicate that the mixing of the Co 3*d* orbitals with the O 2*p* orbitals is relatively strong in $\text{La}_{1-x}\text{Sr}_x\text{CoO}_3$. As for the O 1*s* MCXD signal, the negative finite signals show that $M_{\text{orb}}(\text{O}2p) > 0$. Then the orbital magnetic moment of the O 2*p* orbital is parallel to the orbital magnetic moment of Co 3*d* and the total magnetic moment of $\text{La}_{1-x}\text{Sr}_x\text{CoO}_3$. As in the case of $\text{La}_{1-x}\text{Sr}_x\text{MnO}_3$, the orbital magnetic moment of the O 2*p* orbital is antiparallel to the orbital magnetic moment of Mn 3*d*, which is explained by the mechanism that $M_{\text{orb}}(\text{O}2p)$ is induced by a direct transfer of $M_{\text{orb}}(\text{Mn}3d)$ via strong *d-p* hybridization.²⁸ According to a recent calculation on the TMO_6 cluster model,²⁹ the O 2*p* orbital magnetic moment becomes parallel to the TM *d* orbital magnetic moment when there are holes in the TM *d t*_{2g} states, namely, when the Co 3*d* ion in $\text{La}_{1-x}\text{Sr}_x\text{CoO}_3$ takes the IS state.

IV. CONCLUSION

We have made Co 2*p* and O 1*s* core-level MCXD measurements on $\text{La}_{1-x}\text{Sr}_x\text{CoO}_3$. The Co 2*p* MCXD spectra have been analyzed with use of the orbital and spin sum

rules. The MCXD magnetic moments obtained from the sum rules are compared with the magnetization measurements, showing qualitatively good agreement. From the information about the magnetic moments and the ratio between the orbital magnetic moment and the spin magnetic moment, the intermediate-spin state is suggested to exist in a wide concentration range *x* in $\text{La}_{1-x}\text{Sr}_x\text{CoO}_3$. However, the absolute values for these moments are small compared with the ionic model, indicating the itinerant electron description of the Co 3*d* states may be more appropriate. Negative finite MCXD structures have been observed in the O 1*s* MCXD spectra, indicating the mixing of the O 2*p* orbitals with the Co 3*d* orbitals. The orbital magnetic moment of O 2*p* is shown to be parallel to the orbital magnetic moment of Co 3*d* and to the total magnetic moment, again consistent with the intermediate-spin state of Co 3*d*.

ACKNOWLEDGMENTS

The authors thank A. Fujiwara for help in the SQUID measurements and T. Mizokawa for useful discussions. This work was supported by the New Energy and Industrial Technology Development Organization (NEDO) and a Special Coordination Fund from the Science and Technology Agency. The work at Photon Factory was approved by the Program Advisory Committee (Proposal No. 97G-348)

- ¹M. Abbate, R. Potze, G. A. Sawatzky, and A. Fujimori, *Phys. Rev. B* **49**, 7210 (1994).
- ²A. Chainani, M. Mathew, and D. D. Sarma, *Phys. Rev. B* **46**, 9976 (1992).
- ³R. R. Heikes, R. C. Miller, and R. Mazelsky, *Physica (Amsterdam)* **30**, 1600 (1964).
- ⁴G. H. Jonker and J. H. van Santen, *Physica (Amsterdam)* **19**, 120 (1953).
- ⁵P. M. Raccah and J. B. Goodenough, *Phys. Rev.* **155**, 932 (1967).
- ⁶P. M. Raccah and J. B. Goodenough, *J. Appl. Phys.* **39**, 1209 (1968).
- ⁷G. H. Jonker, *J. Appl. Phys.* **37**, 1424 (1966).
- ⁸K. Asai, O. Yokokura, N. Nishimori, H. Chou, J. M. Tranquada, G. Shirane, S. Higuchi, Y. Okajima, and K. Kohn, *Phys. Rev. B* **50**, 3025 (1994).
- ⁹K. Asai, P. Gehring, H. Chou, and G. Shirane, *Phys. Rev. B* **40**, 10 982 (1989).
- ¹⁰V. G. Bhide, D. S. Rajoria, G. R. Rao, and C. N. R. Rao, *Phys. Rev. B* **6**, 1021 (1972).
- ¹¹M. Abbate, J. C. Fuggle, A. Fujimori, L. H. Tjeng, C. T. Chen, R. Potze, G. A. Sawatzky, H. Eisaki, and S. Uchida, *Phys. Rev. B* **47**, 16 124 (1993).
- ¹²T. Saitoh, T. Mizokawa, A. Fujimori, M. Abbate, Y. Takeda, and M. Takano, *Phys. Rev. B* **55**, 4257 (1997).
- ¹³M. Itoh, I. Natori, S. Kubota, and K. Motoya, *J. Phys. Soc. Jpn.* **63**, 1486 (1994).
- ¹⁴N. Menyuk, P. M. Raccah, and K. Dwight, *Phys. Rev.* **166**, 510 (1968).
- ¹⁵V. G. Bhide, D. S. Rajoria, C. N. R. Rao, G. R. Rao, and V. G. Jadhao, *Phys. Rev. B* **12**, 2832 (1975).
- ¹⁶M. Itoh and I. Natori, *J. Phys. Soc. Jpn.* **64**, 970 (1995).
- ¹⁷T. Taguchi, M. Shimada, and M. Koizumi, *Mater. Res. Bull.* **13**, 1225 (1978).
- ¹⁸H. Taguchi, M. Shimada, and M. Koizumi, *J. Solid State Chem.* **29**, 221 (1979).
- ¹⁹R. H. Potze, G. A. Sawatzky, and M. Abbate, *Phys. Rev. B* **51**, 11 501 (1995).
- ²⁰T. Saitoh, T. Mizokawa, A. Fujimori, M. Abbate, Y. Takeda, and M. Takano, *Phys. Rev. B* **56**, 1290 (1997).
- ²¹C. T. Chen, N. V. Smith, and F. Sette, *Phys. Rev. B* **43**, 6785 (1991).
- ²²C. T. Chen, Y. U. Idzerda, H.-J. Lin, N. V. Smith, G. Meigs, E. Chaban, G. H. Ho, E. Pellegrin, and F. Sette, *Phys. Rev. Lett.* **75**, 152 (1995).
- ²³B. T. Thole, P. Carra, F. Sette, and G. van der Laan, *Phys. Rev. Lett.* **68**, 1943 (1992).
- ²⁴P. Carra, B. T. Thole, M. Altarelli, and X. Wang, *Phys. Rev. Lett.* **70**, 694 (1993).
- ²⁵Y. Teramura, A. Tanaka, and T. Jo, *J. Phys. Soc. Jpn.* **65**, 1053 (1995).
- ²⁶J. Stöhr and H. König, *Phys. Rev. Lett.* **75**, 3748 (1995).
- ²⁷T. Saitoh, A. E. Bocquet, T. Mizokawa, and A. Fujimori, *Phys. Rev. B* **52**, 7934 (1995).
- ²⁸T. Koide, H. Miyauchi, J. Okamoto, T. Shidara, T. Sekine, A. Fujimori, H. Fukutani, S. Kawasaki, M. Takano, and Y. Takeda (unpublished).
- ²⁹A. Tanaka (unpublished).